



Spatio-temporal characteristics of Heat stress over Nigeria using evaluated ERA5-HEAT reanalysis data

Tobi Eniolu Morakinyo^{a,*}, Kazeem Abiodun Ishola^{b,c}, Emmanuel Olaoluwa Eresanya^{b,d},
Mojolaoluwa Toluwalase Daramola^e, Ifeoluwa Adebawale Balogun^f

^a School of Geography, University College Dublin, Ireland

^b Irish Climate Analysis Research Units (ICARUS), Department of Geography, Maynooth University, Co. Kildare, Ireland

^c National Centre for Geocomputation, Maynooth University, Ireland

^d Organization of African Academic Doctors (OAAD), Langata, Nairobi P.O. Box 14833-00100, Kenya

^e Institute of Geographic Sciences and Natural Resources Research, Chinese Academy of Sciences, 11A Datun Road, Beijing, 100101, China

^f Department of Meteorology and Climate Science, Federal University of Technology, Akure, Nigeria

ARTICLE INFO

Keywords:

Heat stress
Thermal comfort
ERA5-HEAT
Nigeria
Africa
UTCI

ABSTRACT

Nigeria's growing population faces an increasing heat burden with potential health risks. The Universal Thermal Comfort Index (UTCI) links outdoor conditions and human well-being but lacks comprehensive *in situ* data in developing regions like Nigeria. ERA5-HEAT reanalysis offers a solution with gridded UTCI and MRT data, but validation is crucial. Thus, this study evaluates the ERA5-HEAT UTCI against data from nine Nigerian weather stations and analysed the spatio-temporal patterns of heat stress trends. Results showed that ERA5-HEAT demonstrated reasonable statistical performance and captured the temporal characteristics and patterns of UTCI across Nigeria's climatic zones. Seasonal variations show heat stress levels from "slightly cold" to "moderate" at 0600 LST and "moderate" to "very strong" at 1500 LST. Geographical consistency exists within each season over the decades, with a critical "very strong" heat stress period during March-May. Additionally, there has been an increasing spatial expansion of areas experiencing higher heat stress levels across the country. Latitudinally, stable patterns exist across decades at 0600 LST for each season. Seasons show distinct UTCI values, and at 1500 LST, more variability and category transitions occur along latitudes. Furthermore, the results indicate significant positive trends and occasional non-significant negative trends over the 40-year period. Notably, during 0600 LST, the Guinea and Sahel regions exhibit relatively higher positive trends than the Sudan region in all seasons, whereas at 1500 LST, high positive trends are prominent in DJF and MAM seasons, indicating increased heat stress during peak seasons. These positive deviations in UTCI are associated with adverse effects on human health, including increased mortality rates.

1. Introduction

1.1. Background of study

The escalating global warming has given rise to critical temperature-related challenges, including heatwaves, heat stress, and thermal discomfort which are projected to increase in magnitude and frequency (Adelekan et al., 2022). Coupling the global warming and consequent effects is the challenge of the rapid pace of urbanization, driven by the increasing global population and a rising rate of rural-urban migration. Currently, over half of the global population resides in urban areas, a

percentage projected to increase to 68% by 2050 (UNDESA, 2019). This substantial urbanization has given rise to the urban heat island effect, where urban temperatures significantly exceed those in suburban areas, particularly during nighttime (Okeahialam, 2016; Santamouris, 2015). This phenomenon exacerbates heatwaves in urban areas, and results in heightened levels of heat stress, consequently diminishing the quality of urban living in numerous cities worldwide.

Driven by both high population growth and extreme temperatures, sub-saharan Africa's exposure to dangerous heat during the 21st century is the highest among all regions globally (Parkes et al., 2022; Tuholske et al., 2021; Eresanya et al., 2018). This has been projected to increase

* Corresponding author.

E-mail address: tobi.morakinyo@ucd.ie (T.E. Morakinyo).

<https://doi.org/10.1016/j.wace.2024.100704>

Received 6 November 2023; Received in revised form 14 May 2024; Accepted 10 June 2024

Available online 15 June 2024

2212-0947/© 2024 The Author(s). Published by Elsevier B.V. This is an open access article under the CC BY license (<http://creativecommons.org/licenses/by/4.0/>).

substantially, from 2 billion person-days per year in 1985–2005 to 45 billion person-days by the 2060s at 1.5 °C global warming and low population growth. At 2.8 °C global warming and medium-high population growth, the projection indicate an increase to 95 billion person-days, with the greatest exposure projected in West Africa where Nigeria, this study geographic area is located (Trisos et al., 2022). Moreover, the escalating population in this region implies high exposure to extreme heat stress conditions, and consequently heat-related morbidity and mortality though unreported or under-reported (Ame-gah et al., 2016).

The interplay of high temperatures with other weather parameters, such as humidity, wind speed, and solar radiation, results in varying degrees of human thermal stress and comfort (Morakinyo et al., 2019). This complex phenomenon, known as heat stress, challenges the human body's ability to maintain its core temperature within the range required for optimal comfort, performance, and health (Di Napoli et al., 2021a; Ncongwane et al., 2021). Heat stress has multiple adverse effects on human health, livelihood, and productivity, particularly in terms of health-related impacts and risks resulting in morbidity and mortality (Ncongwane et al., 2021; Pasquini et al., 2020). Over 5 million deaths per year have been attributed to non-optimum temperatures, especially among vulnerable population groups (Zhao et al., 2021).

1.2. Thermal studies in Nigeria: trends, patterns and applied indices

Research on heat or thermal stress in Nigeria has been ongoing for approximately four decades, with pioneering work by Ayoade (1978) and Olaniran (1982). These early studies laid the foundation for assessing thermal stress conditions in Nigeria using indicators or indices such as Air Temperature (AT), Wet-Bulb Temperature (WBT), Temperature-Humidity Index (THI), and Effective Temperature Index (ETI). For example, Ayoade (1978) employed the ETI to depict physiologic comfort zones across Nigeria, recognizing four distinct zones. Building upon Ayoade's work, Eludoyin and Adelekan (2013) conducted a climatological study of thermal stress in Nigeria from 1951 to 2009, employing temperature and humidity-based indices such as THI, Relative Strain Index (RSI) and ETI. These studies revealed associations between ecological zones and physiologic thermal zones, with the montane region identified as having the most comfortable physiologic climate and regions around the Rivers Niger and Benue troughs as the most uncomfortable for most of the year. They also observed a significant increase in physiologic stress in Nigeria from 1981 to 2009 compared to the period from 1951 to 1980. Subsequent studies have leveraged these indices to investigate and characterize thermal stress conditions at various spatial scales, as demonstrated by research conducted by (Eludoyin, 2014).

While temperature and humidity are essential components of thermal or heat stress, the influence of radiation and wind cannot be underestimated. Recent studies, e.g Omonijo (2017) and Omonijo et al. (2013) applied energy/radiation-based human comfort indices like Physiological Equivalent Temperature (PET) and Universal Thermal Comfort Indices (UTCI) to analyze thermal stress conditions in Nigeria, however, their geographic coverage of studies was limited to Ondo and Oyo states in South-Western Nigeria. This could be partly due to common challenges of limited availability of weather stations, and where available, limited accessibility to requisite data. Climate Research in Nigeria often relies on weather data from the Nigeria Meteorological Agency (NIMET) and other sources, such as state ministries of environment and agriculture, research institutes and higher education institutions, which have a sparse distribution of synoptic weather stations across the region. Given the constraints of observation stations, a comprehensive characterization of thermal stress in Nigeria using an human energy-balance based thermal index such as UTCI is lacking. Meanwhile the application of such an index could accurately reflect the heat perception of the populace given the tropical location of the country where a high amount of radiation is received across the year.

Leveraging the freely available, temporally consistent, and spatially comprehensive ERA5-HEAT reanalysis data can help bridge this gap. Nonetheless, assessing the accuracy and potential biases of reanalysis data remains essential which is yet to be explored in the Nigerian context. The sub-section below discusses ERA5-HEAT and its utilization to understand heat stress/thermal comfort in specific regions around the world.

1.3. Recent application of ERA5-HEAT reanalysis for heat stress studies

Recently, the European Centre for Medium-Range Weather Forecasts (ECMWF) has produced advanced spatially gridded historical records of UTCI and MRT (Mean Radiant Temperature), known as ERA5-HEAT (Human thErMAl comfOrT) (Di Napoli et al., 2021a). These datasets consist of hourly UTCI and MRT, presented on a 0.25° x 0.25° spatial grid, spanning from 1940 to the present. These datasets are derived from atmospheric variables sourced from ERA5 reanalysis data, including 2-m air and dew-point temperature for relative humidity, 10-m zonal and meridional winds for wind speed. In addition, the MRT is calculated using solar and thermal radiation fluxes, as outlined in Di Napoli et al. (2018). Thermal radiation encompasses both the downwelling thermal component from the atmosphere and the upwelling thermal component from the ground. Solar radiation consists of a direct component from the sun and a diffuse component, where the latter comprises the sum of isotropic diffuse solar radiation flux and surface-reflected solar radiation flux (Di Napoli et al., 2023). The resulting MRT, a crucial parameter in assessing human response to radiant effects are then integrated with other atmospheric data to compute UTCI using the Fiala model, following established operational procedures (Bröde et al., 2012; Fiala et al., 2012). UTCI serves as a widely accepted indicator of human thermal stress, created from climate variables such as air temperature, wind, humidity, and radiation. It is a biometeorological index used for evaluating the health impacts of climate conditions related to heat (Di Napoli et al., 2018). The ERA5-HEAT UTCI has been widely evaluated and applied in different countries and regions (Antonescu et al., 2021; Brimicombe et al., 2021; Di Napoli et al., 2023; Kyaw et al., 2023; Miranda et al., 2023; Roffe et al., 2023; Shukla et al., 2022; Urban et al., 2021; and Zare et al., 2018).

Miranda et al. (2023) analysed heat stress patterns in South America using ERA5-HEAT data from 1979 to 2020. They focused on 31 populous cities, observing more heat stress hours inland compared to coastal areas. The annual count of heat stress hours increased significantly from 1979 to 2020, with varying rates. Extreme heat events surged, particularly after 2000. Urban et al. (2021) conducted a comparative study across Europe, evaluating the potential of ERA5-based UTCI to identify life-threatening thermal conditions where station data are scarce. They analysed 21 cities in 9 European countries. While they found similarities in heat and cold effects in most locations, the study highlighted the significant influence of wind on UTCI, especially in southern Europe. Kyaw et al. (2023) examined heat stress patterns in South Asia from 1979 to 2021 using ERA5-HEAT UTCI data. Their study revealed significant regional variations. Bangladesh in the east showed the highest mean UTCI range (26–32 °C), while Afghanistan had the lowest. In the west, along the India-Pakistan border, the daily maximum UTCI range was the highest (38–46 °C). The research also indicated increasing mean and maximum UTCI levels, with a 0.25 to 0.75 °C per decade rise in Pakistan, Afghanistan, and northwest India, particularly during June to September.

Shukla et al. (2022) analysed heat stress in northwest India using the ERA5-HEAT dataset from 1981 to 2019. Their findings revealed that this region experienced stronger heat stress with a monthly and seasonal mean UTCI ranging from 27 to 34.5 °C, notably higher than other areas in India (below 25.5 °C). The peak heat stress occurred in June (34.5 °C) and July (33.5 °C) due to elevated soil temperatures and significant sensible heat fluxes. The study highlighted the impact of strong westerly winds from the Arabian Sea, carrying substantial moisture, on the high

thermal stress. Importantly, both North-west India and the entire country showed significant rising trends in seasonal mean UTCI ($0.9\text{ }^\circ\text{C}$ per 39 years and $0.6\text{ }^\circ\text{C}$ per 39 years, respectively), indicating a faster increase in thermal discomfort in these regions compared to the rest of India.

Over sub-saharan Africa, ERA-HEAT UTCI data have been applied by very limited studies. For instance, [Guigma et al. \(2020\)](#) conducted a comparative analysis of Sahelian heatwaves, examining their characteristics and thermodynamics using various thermal indices such as temperature (T), heat index (HI), Steadman non-radiant Apparent Temperature (AT), Net Effective Temperature (NET), and Universal Thermal Comfort Index (UTCI). Their findings revealed sensitivity of thermodynamic processes characterizing heatwaves and resulting heat stress to the choice of indices. In regions of the southernmost Sahel with low index similarity, emphasis on humidity-weighted indices like HI, AT, and UTCI is crucial, given the significant moisture variability, particularly during April-May-June. Conversely, in Northeastern Sahel and the broader domain during February-March, where environmental variable variability is minimal, the added value of complex indices like UTCI in heat warnings is limited. Another study applied it to understand the spatio-temporal pattern of heat stress in Southern Africa from 1979 to 2021 at different time scales ([Roffe et al., 2023](#)). They found that spatially, there's widespread absence of heat stress in daily mean values, but daily maximum and minimum values exhibit significant heat and cold stress incidents, including moderate and strong heat stress and slight to moderate cold stress. The study also highlights the impact of El Niño and La Niña phases on heat stress during summer, with El Niño intensifying heat stress and La Niña reducing it. Overall, there's a notable increase in heat stress over the study period, particularly during spring and summer, with some regions experiencing decreasing trends. In South Africa, [Havenga et al. \(2022\)](#) utilized long-term ERA5-HEAT UTCI data to examine heat stress during the traditional Comrades Marathon, previously held in the austral winter (May-June), compared to a new period in the austral spring (end of August). Their findings reveal a higher likelihood of participants being exposed to 'strong' and 'very strong' heat stress periods if the event is scheduled for August, as opposed to the original dates. Only a few studies have applied UTCI for impact research. [Bonell et al. \(2022, 2023\)](#) explored the impact of heat stress on child and maternal health in the Gambia using UTCI. They aimed to ascertain whether environmental heat stress affects fetal physiology in pregnant subsistence farmers. Their findings indicated a 1.05-fold increase in the likelihood of pre-term birth for every $1\text{ }^\circ\text{C}$ above average, suggesting that reducing maternal exposure to heat stress could alleviate fetal strain and potentially mitigate adverse birth outcomes. Furthermore, studies have consistently observed lower birth weights associated with exposure to extreme heat, particularly among mothers from lower socioeconomic backgrounds ([Bonell et al., 2023](#)). While the reanalysis product has been applied across geographies, it's been mostly used as an alternative to observation in most cases. Very limited studies, for instance, [Krüger and Di Napoli \(2022\)](#) has evaluated the product's parameters against observations.

Therefore, this study conducts an investigation into the spatio-temporal patterns and trend of heat stress over Nigeria by utilizing ERA5-HEAT and observational datasets. The specific objectives are to: (1) evaluate the performance of ERA5-HEAT UTCI against observational data from nine weather stations distributed across three distinct ecoclimatic zones in Nigeria; 2) analyze the long-term annual and seasonal spatio-temporal trends of ERA5-HEAT UTCI across Nigeria to provide insights into how thermal stress and exposure have evolved over time; 3) identify potential latitudinal long-term shifts or changes of observed thermal zones within Nigeria to better understand how the thermal landscape in Nigeria has transformed over the years, 1981–2020.

2. Methodology

2.1. Study area - geography of Nigeria

Nigeria, located in the western part of Africa, lies between 4 and 14°N latitude and 3 - 14°E longitude. It is bounded by the Republic of Benin to the west, Niger to the north, Cameroon to the east and the Gulf of Guinea towards the south. The total land area covers about $923,770\text{ km}^2$ making it one of the largest countries in Africa. Nigeria has a wide variety of landscapes and landforms. The northern part is characterized by vast savanna grasslands and scattered shrubbery and trees, while Mangrove swamps and low-lying plains characterize the southern region ([Oluleye and Adeyewa, 2016](#)). Plateaus and hills are prevalent in the central part of the country, with notable ones like the Jos plateau ([Fig. 1](#)). It has three distinct climate zones: a tropical monsoon climate in the south, a tropical savannah climate characterizing its central parts, and a hot, semi-arid Sahelian climate in the north ([World Bank, 2021](#); [Omotosho and Abiodun, 2007](#)). Nigeria in her a tropical location experiences wet and dry season. The seasons are driven by the periodic northward and southward migration and retreat of the Inter-Tropical Convergence Zone (ITCZ), defined by the tropical maritime (mT) from the Atlantic Ocean and the tropical continental (cT) airmass ([Gbode et al., 2019](#); [Eludoyin and Adelekan, 2013](#)). The northward migration of the ITCZ defines the wet season, a period of intense convective activity over the country, mostly across the southern region. The precipitation pattern exhibits a latitudinal gradient, with more precipitation occurring in the southern parts and decreases northwards ([Akinsanola and Ogunjobi, 2014](#)).

2.2. Description of observed meteorological data and stations

In this study, we obtained observation data from nine Nigerian Meteorological Agency (NIMET)'s weather stations across the country and across the three latitudinal subdivisions i.e. Guinea (coast - 8°N), Sudan (8°N – 11°N) and Sahel (11°N – 16°N) ([Omotosho and Abiodun, 2007](#)). This zonal subdivision was used in the study by [Balogun et al. \(2019\)](#), who assessed the bioclimatic conditions across Nigeria at 0600 and 1500 Local Standard Time (LST). The data obtained from the stations includes the monthly averages of air temperature ($^\circ\text{C}$), wind speed (m/s), relative humidity (%) at 0600 and 1500 LST from 1981 to 2010. Nevertheless, it's crucial to note that while global radiation is zero at 06:00 LST, the 15:00 LST global radiation was extrapolated from monthly mean data using a multiplication factor derived from the

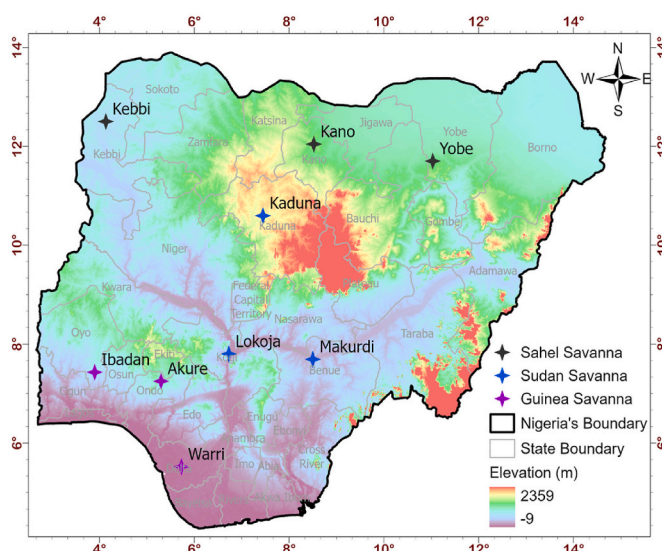


Fig. 1. Map of Nigeria and location of NiMET synoptic weather stations.

mean-max ratio over Ile-Ife, Nigeria (Soneye et al., 2019). 0600 and 1500 LST, are considered two distinct periods when solar insolation was minimal and maximum, respectively. This was considered in the evaluation of the reanalysis-derived thermal indices. Due to several factors, such as the completeness of the data within the period 1981–2010, limited data access and data quality, we followed the selection of three stations within each zone. We checked the data for missing values and filtered out outliers assumed to be due to errors.

2.3. Method of analysis

This section elaborates on the methods adopted to achieve the objectives of this study. To assess the performance of ERA5-HEAT UTCI, data was collected at 0600 and 1500 LST spanning from 1981 to 2020. These specific hours were chosen to align with the in-situ station data (as described in section 2.2) and provide an adequate representation of distinct time periods in a day: early morning (minimum) and afternoon (maximum) heat stress levels experienced during the day, as previously discussed by Balogun et al. (2019) and Kyaw et al. (2023). The sub-section below details the methods used to calculate UTCI based on observed data, evaluate performance, and conduct spatio-temporal analysis.

2.3.1. UTCI calculation based on observed data

The UTCI at each weather station was estimated using the RayMan model (Matzarakis et al., 2007, 2010), which was developed for the calculation of the MRT and thermal indices, including UTCI, in both simple and complex environments. The model relied solely on data of air temperature, air humidity, wind speed and MRT. While the first three parameters obtained from the weather stations are directly fed into the model, to determine the MRT, shortwave and longwave radiation fluxes affecting the human energy balance were calculated by the model based on the supplied global radiation data. In Rayman, MRT is calculated based on globe-thermometer method following the guidelines set by the German VDI-Guideline (VDI, 1998) and assumed a sky view factor (SVF) of 1, which corresponds to an open field typical of WMO standard weather stations. This excludes the effects of the shading caused by building structures on direct and diffuse radiation. In RayMan, the UTCI is estimated via a regression equation based on a heat transfer model (Fiala et al., 2012; Fröhlich et al., 2019) which accounts for the aforementioned meteorological variables as measured at the NIMET weather stations.

2.3.2. Performance evaluation of ERA5-HEAT UTCI

The performance evaluation involved subsetting the global ERA5-HEAT data to obtain spatial UTCI values over Nigeria for specific hours at 0600 and 1500 from 1981 to 2010. To match the temporal resolution of local observation data, the data for each grid cell was separately aggregated into monthly averages for the performance evaluation analysis. To assess ERA5-HEAT against reference (RayMan) UTCI values, monthly gridded UTCI values were extracted for grid cells overlapping with station locations. These extracted values were then compared directly to in-situ UTCI values from 1981 to 2010 for each station. Additionally, UTCI values for each climate zone (Guinea, Sudan, and Sahel) were compared. The performance of ERA5-HEAT was further evaluated using specific error statistics, including the Root Mean Square Error (RMSE), Mean Bias Error (MBE), Pearson Correlation Coefficient (R), and the RMSE-Standard Deviation Ratio (RSR). The RSR helps to effectively constrain uncertainty in gridded ERA5-HEAT data.

The metrics are calculated as,

$$RSR = \frac{RMSE}{SD_{ref}} = \frac{\sqrt{\frac{\sum_{i=1}^n (UTCI_i^{ref} - UTCI_i^{ERA5-HEAT})^2}{n}}}{\sqrt{\frac{\sum_{i=1}^n (UTCI_i^{ref} - \overline{UTCI_i^{ref}})^2}{n}}} \quad (1)$$

$$MBE = \frac{1}{n} \sum_{i=1}^n (UTCI_i^{ERA5-HEAT} - UTCI_i^{ref}) \quad (2)$$

$$R = \frac{\sum_{i=1}^n (UTCI_i^{ref} - \overline{UTCI_i^{ref}}) (UTCI_i^{ERA5-HEAT} - \overline{UTCI_i^{ERA5-HEAT}})}{\sqrt{\sum_{i=1}^n (UTCI_i^{ref} - \overline{UTCI_i^{ref}})^2 \sum_{i=1}^n (UTCI_i^{ERA5-HEAT} - \overline{UTCI_i^{ERA5-HEAT}})^2}} \quad (3)$$

where SD is the standard deviation, ref is the reference datasets, i is the month, n is the total number of months in the analysis period, The bar accent is the long-term monthly mean (1981–2010) of the reference data and ERA5-HEAT UTCI. The values of RSR range from 0 for zero RMSE, indicating perfect ERA5-HEAT, to large positive values, indicating imperfect ERA5-HEAT UTCI values.

2.3.3. Spatial trend and decadal shift analysis methodology

The spatial and temporal trend characteristics of ERA5-HEAT UTCI at 0600 and 1500 LST are further analysed. First, the UTCI values per grid cell are delineated and classified into broad thermal categories following Błażejczyk et al. (2013) (Table 1). Thereafter, some dimensions of long-term spatio-temporal characteristics and analysis were explored. For instance, we analysed potential spatial variation of thermal classes on a decadal basis. Also, a latitudinal shift analysis of decadal UTCI was performed where the UTCI thermal classes are aggregated separately for four decades, 1981–1990, 1991–2000, 2001–2010 and 2011–2020, and compared with reference to the earliest decade 1981–1990; and over each zone by aggregating the grid cell values over a constant longitudinal band (2–15° E). These assessments are carried out aggregately for each of the four seasons namely December-February (DJF i.e. preceding year “D” with current year “J” and “F”); March-May (MAM), June-August (JJA), September-November (SON) and at annual scale.

It should be noted that the seasons in Nigeria vary across regions, influenced by the periodic shift in the position of ITCZ. For example, dry periods (DJF) are common across the country, but the Guinea zone experiences two wet seasons, one from March to July and the other from September to October (Adegoke and Ajayi, 2015). In contrast, the Sahel experiences just one wet period from June to September. Due to this mismatch, we are sticking to the traditional periods that are commonly used for seasonal analysis (e.g Adeyeri and Ishola (2021); Omotosho and Abiodun (2007)). Lastly, the areal coverage of each spatially dominated thermal class per month is extracted and further analysed separately for 0600 and 1500 LST. In a similar vein, percentage of grid cells of seasonal, annual and decadal composite UTCI values for the dominant thermal categories are analysed using cumulative frequency analysis in order to efficiently quantify the proportion of grid cells dominated by the ERA5-HEAT UTCI range, and also helps to determine whether or not the proportion of a UTCI category has changed spatially during the study period. Thereafter, the trends in ERA5-HEAT UTCI values are calculated

Table 1
Thermal comfort/Heat stress classification based on UTCI value.

UTCI range (° c) ^a	Level of thermal stress
<- 40	extreme cold stress
-40 to -27	very strong cold stress
-27 to -13	strong cold stress
-13 to 0	moderate cold stress
0-9	slight cold stress
9-26	no thermal stress
26-32	moderate heat stress
32-38	strong heat stress
38-46	very strong heat stress
>46	extreme heat stress

^a Błażejczyk et al. (2013).

over the same spatial extent and resolution, using nonparametric Mann-Kendall trend test and Sen's slope estimator (Adeyeri and Ishola, 2021; Kendall, 1948; Mann, 1945; Sen, 1968). This is done across all the seasons and annual for 0600 and 1500 LST, using the 'raster.kendall' function in the 'spatialEco' R library (Evans et al., 2020).

3. Results and discussion

3.1. Comparative data description & performance evaluation of ERA5-HEAT UTCI over Nigeria

3.1.1. Comparative description of observed and ERA5-HEAT UTCI

Despite the remarkable achievements of producing the ERA5-HEAT datasets and its usefulness in addressing the problems of paucity of data across the globe, uncertainties due to inherent errors associated with ERA5 input variables such as the radiation components exists (Di Napoli et al., 2021a) as with other reanalysis products. Therefore, effective use of ERA5-HEAT in different regions requires adequate evaluation of its performance, instead of or before treating the products as observations.

First, we illustrated and discussed the density distribution of ERA5-HEAT UTCI values in comparison with reference (observed) datasets for each region (see Fig. 2). At 0600 LST (morning), UTCI values for both sources are densely distributed in no thermal stress category 9–26 °C, with small variance and median values (black crossbar) of about 24 °C for observed and 25 °C for ERA5-HEAT, in Guinea region. While a large proportion of UTCI values in the Sudan and Sahel are also distributed in no thermal stress category with less median UTCI values, there is a relatively large variance in both data sources. The UTCI values extend beyond 0 °C in some instances, indicating occasional slight to moderate cold stress for these regions. The evidence of cold stress during 0600 LST in the Sudan and Sahel occur mostly in the Harmattan winter (DJF) season when the atmospheric condition is dominated by large-scale strong north-easterly trade winds that drive the meeting of dry and dusty surface of the Sahara with the cold airmass from the midlatitude, yielding a cold-dusty wind condition, in addition limit insolation at this time (Okeahialam, 2016). This is similar to the reports in previous studies (e.g. Eludoyin, 2014; Eludoyin et al., 2014) using Relative Strain Index (RSI) and Temperature Humidity Index (THI) which demonstrate that before 0600 and after 2100 LST, the Northern Nigeria for which the

Sudan and Sahel are characterised, experiences cold stress, particularly during December Harmattan period.

At 1500 LST, UTCI values are largely distributed between “moderate” and “strong” heat stress in the Guinea zone, but the upper limit extends up to the “very strong heat stress” category for the Sudan and Sahel zones. Though there are observed disparities in the median UTCI values and the mean distribution between observed and ERA5-HEAT is statistically significant ($\alpha < 0.05$) particularly in Sudan and Sahel, the broad UTCI values between both sources are generally comparable and effectively within the same thermal categories. In essence, ERA5-HEAT reproduces UTCI values that are fairly consistent with the reference datasets across Nigeria, notwithstanding the spatial scale difference between the station and ERA5-HEAT.

Comparatively, the Sudan and Sahel regions have a relatively higher thermal stress category than Guinea during the hottest afternoon, due to higher mean radiant temperature partly associated with higher insolation and temperature in these regions. A synergistic influence of high temperature and atmospheric moisture, exposure to insolation and poor ventilation has been reported as the major contributors to heat accumulation in the human body (McGregor and Vanos, 2018). While this study does not evaluate the drivers of UTCI variations, Di Napoli et al. (2023) demonstrates that the combined decrease of 2-m temperature, relative humidity and high wind speed drives low UTCI in the Caribbean. These characteristics are evident for 0600 LST during which the UTCI values are slightly lower for Sudan and Sahel than for Guinea.

The higher thermal stress during 1500 than 0600 LST across the region is typical of tropical regions where heat accumulates during the day shortly after the peak of insolation, usually at noon. Previous studies in the tropical region (Kyaw et al., 2023; Morakinyo et al., 2019) have shown that human thermal discomforts occur during the peak of heat and temperature around 1500 LST. This is further supported by Runnalls and Oke (2000) who reveal afternoon has the maximum heat conditions and morning or nighttime as the best human thermal condition. In the context of Nigeria, Eludoyin (2014) also demonstrates that the period between 1200 and 1500 LST is thermally stressful in Nigeria. While identifying the best human thermal condition is beyond the scope of this study, our results are broadly consistent with previous studies, as evidently illustrated in Fig. 2.

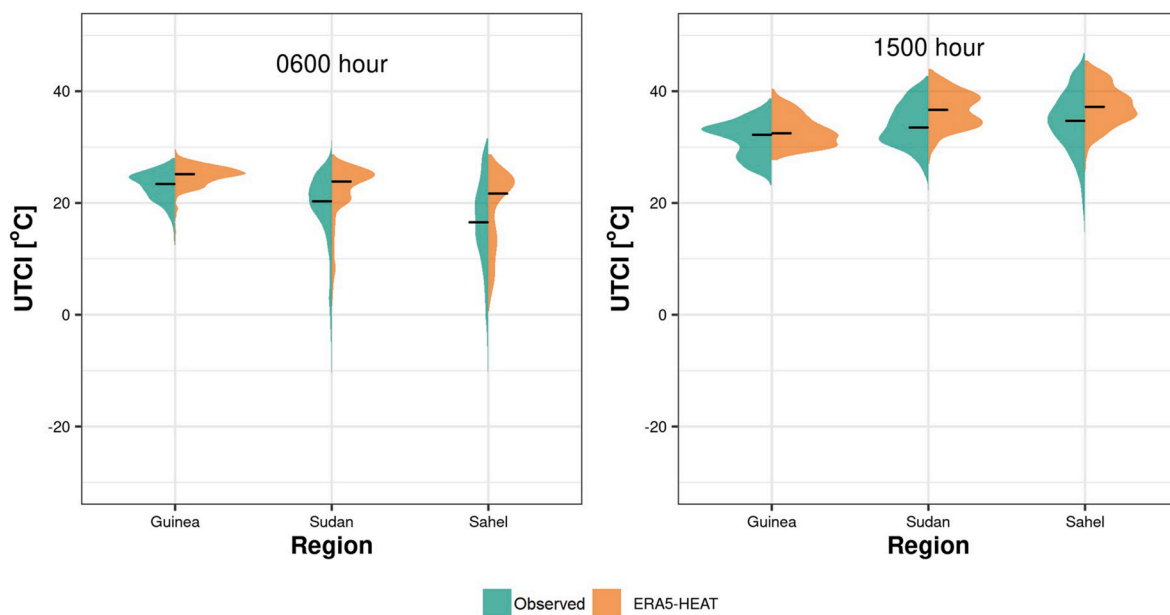


Fig. 2. Comparison between ERA5-HEAT and observed (calculated with RayMan) monthly UTCI distribution across stations, grouped into three geographical zones (Guinea, Sudan and Sahel), over the period 1981–2010 for 0600 and 1500 LST.

3.1.2. Performance evaluation of ERA5-UTCI over Nigeria

The results of performance statistics of ERA5-HEAT for each station and cumulatively for each region are presented in Fig. 3 while the line plot for each station at 0600 and 1-500 is shown in Figure A1 and A2, respectively and the regional scattered plots at both times are shown in Fig. 4. ERA5-HEAT shows varying performance across stations and regions. For example, the product performs best at Warri station (located in the Guinea zone), with the lowest RMSE of 1.47 and 1.64 °C, MBE of 1.21 and 0.61 °C at 0600 and 1500 LST, respectively. ERA5-HEAT also performs relatively well in other stations based on the error statistics results especially at 1500 LST. However, the relatively higher errors were observed which might be due to large missing data in the reference datasets in the case of Ibadan at 0600 LST (see Fig. A1, A2). The performance is also low in Kano and Yobe both in the Sahel zone, where ERA5-HEAT largely overestimates or misrepresents the UTCI values especially in the morning (Figures A1,A2).

At regional scales, ERA5-HEAT performs best in the Guinea region, followed by Sudan while Sahel shows the lowest performance during the analysis period (see Figs. 3 and 4). Whereas the products are better for 1500 LST than 0600 LST, likely due to a better representation of physical drivers, particularly mean radiant temperature (see Fig. A3), the errors for both periods are generally well below the uncertainty values that have been previously reported for some stations across the globe (Di Napoli et al., 2021a). Overall, the reference UTCI values for the coldest and hottest times are sufficiently captured by ERA5-HEAT through the analysis period (Fig. 4). Therefore, the product demonstrates reasonable performance in capturing patterns and the spatial and temporal characteristics of human thermal and heat stress conditions across Nigeria.

3.2. Long term spatio-temporal variation of UTCI over Nigeria

This section discusses the results of long-term spatio-temporal variation of UTCI over Nigeria between 1981 and 2020. To further understand the temporal changes, we divided the datasets by decades i.e. 1981-1990, 1991-2000, 2001-2010 and 2011-2020 across seasons: Dry (DJF), pre-Wet (MAM), Wet (JJA) and pre-Dry (SON), for early morning (0600 LST) and afternoon (1500LST) times.

3.2.1. Long-term pattern of minimum UTCI over Nigeria

The spatial characteristics of decadal mean ERA5-HEAT UTCI across the seasons for 0600 LST are presented in Fig. 5. The results show varying thermal stress categories in space and seasons. For the DJF season, moderate heat stress (MHS) covers the south of Guinea, mostly along the coast of Atlantic Ocean, whereas, slight cold stress (SLCS) dominates the Sahelian region. The regional difference in thermal categories between Guinea and Sahel is distinguished by the differing influence of localized phenomenon. Due to its proximity to the Atlantic ocean, the Guinea coast is subject to relative high atmospheric humidity and air temperature consequently modifying the microclimate of the region with high thermal stress, even during the DJF season (Eludoyin, 2014; Eludoyin and Adelekan, 2013). However, the Sahelian region is majorly influenced by strong large-scale northeasterly trade winds that bring cold air mass from the mid-latitude during this season. Similar pattern of MHS for the Guinea region is also observed for SON season and annual scale, and this is consistent for each decade within the study period.

For other seasons, the thermal condition ranges from “No thermal stress (NTS)” and “moderate heat stress (MHS)” across regions, albeit with different patterns of coverage. For instance, during the MAM mornings, NTS prevailed over the Sahel and Sudan whereas MHS was dominant in the Guinea region. The NHS prevailed over the entire country in the JJA mornings except in the North-eastern states like Borno, Adamawa and Gombe state where MHS were observed. Similarly, the NHS prevailed over Sudan, Sahel and Guinea at SON except for the coastal states (Cross River, Akwa Ibom, Bayelsa and Lagos) and Adamawa where the MHS was observed.

Overall, while the NTS category covers the large part of the country in all seasons during 0 600 LST (Fig. 5), the MHS category is more widespread in Guinea and some parts of Sudan region for MAM season. Patches of MHS are also observed in the Northeast of the country for JJA. Notably, some NTS areas in the Guinea, Sudan and Northeast in the early decades (1981-1990) have shifted to MHS in recent decades (2011-2020). This positive shift in the thermal stress category over the 40-year period is broadly eastwards, particularly in the Sudan for MAM season and Guinea for SON, DJF and annual. It further suggests a rising trend in UTCI drivers, especially air temperature, likely associated with increasing global warming and climate change. Fig. 6 illustrates and quantifies the changes in the spatial coverage and cumulative frequency of grids of each dominant thermal stress category over the study period. It shows that while the proportion of area coverage of SLCS is broadly consistent over the years, the proportion of grids for NTS has considerably reduced from 80 to 95% in 1981-1990 to 60-85% in recent years. This is compensated by the increase in the proportion of areas covered by MHS. Further, the cumulative frequency curve (Fig. 6) shows that the Guinea in DJF and SON, and Sudan in MAM have a major decrease and increase in the coverage of NTS and MHS, respectively.

3.2.2. Long-term pattern of maximum UTCI over Nigeria

The peak time (1500 LST) UTCI distribution reveals evident “moderate heat stress” (MHS), “strong heat stress” (SHS) and “very strong heat stress” (VSHS) over the country (see Fig. 7). However, the spatial pattern differs across seasons and decades. In DJF, the VSHS thermal condition is dominant in the Sudan except in Kaduna state where SHS was observed with the same dominant over the Guinea and Sahel zones. During the peak heat stress season i.e. MAM, VSHS and SHS were dominant in the Sahel-Sudan and Guinea respectively. Whereas, during SON and JJA, SHS prevailed in the most part of the country with signatures of MHS in the Guinea region and VSHS in upper Sahel. Overall, the VSHS and MHS coverage increases and reduces over Sudan and Guinea across decades, respectively. For JJA, SON and on an annual scale, VSHS covers the northern Sahel, MHS in the Guinea region, and the rest of the country is dominated by SHS. Regions around the Rivers Niger and Benue troughs as the most uncomfortable for most of the year as also found by Eludoyin and Adelekan (2013). Notwithstanding the seasons, a close observation indicates that the North-central and eastern Sudan region, are relatively characterised by lower thermal stress categories, which are apparently different from the rest of the Sudan-Sahel regions. These areas are majorly characterised by high topography (Fig. 1) such as the Jos and Mambilla Plateau, suggesting the effect of the landscapes on the local thermal stress conditions of the area (Eludoyin, 2014; Ogbonna and Harris, 2008). Additionally, the overarching atmospheric dynamics significantly influence the spatial distribution of heat stress across West Africa in general, manifesting distinct characteristics in various seasons (DJF, MAM, JJA, SON) and between morning and afternoon periods. During the dry season (DJF), the Harmattan wind, originating from the northeast, induces cold stress by transporting cool and dry air from the midlatitude. Nevertheless, in the afternoon, the absence of cloud cover and the consequent maximum solar radiation reaching the Earth’s surface intensify heat stress (Guigma et al., 2020). In the pre-monsoon season (MAM), escalating temperatures and humidity levels, due to influx of moist maritime air from the Atlantic Ocean prompted by the northward shift of the ITCZ, culminate in heightened heat stress, especially during the afternoon, as the region transitions to the wet season (Nikulin et al., 2012). Throughout the wet season, the West African Monsoon (WAM) brings convective activities i.e. cloud cover and precipitation, relatively reducing the intensity afternoon heat stress (Nicholson, 2013). In the post-monsoon season (SON), despite declining temperatures, lingering humidity levels contribute to sustained heat stress levels before dissipating in the afternoon (Sultan et al., 2003). Overall, the variations in thermal stress characteristics are due to the interactions among the local geography (e.g. relief), nearness to waterbody, large-scale wind patterns, and high relative humidity and air

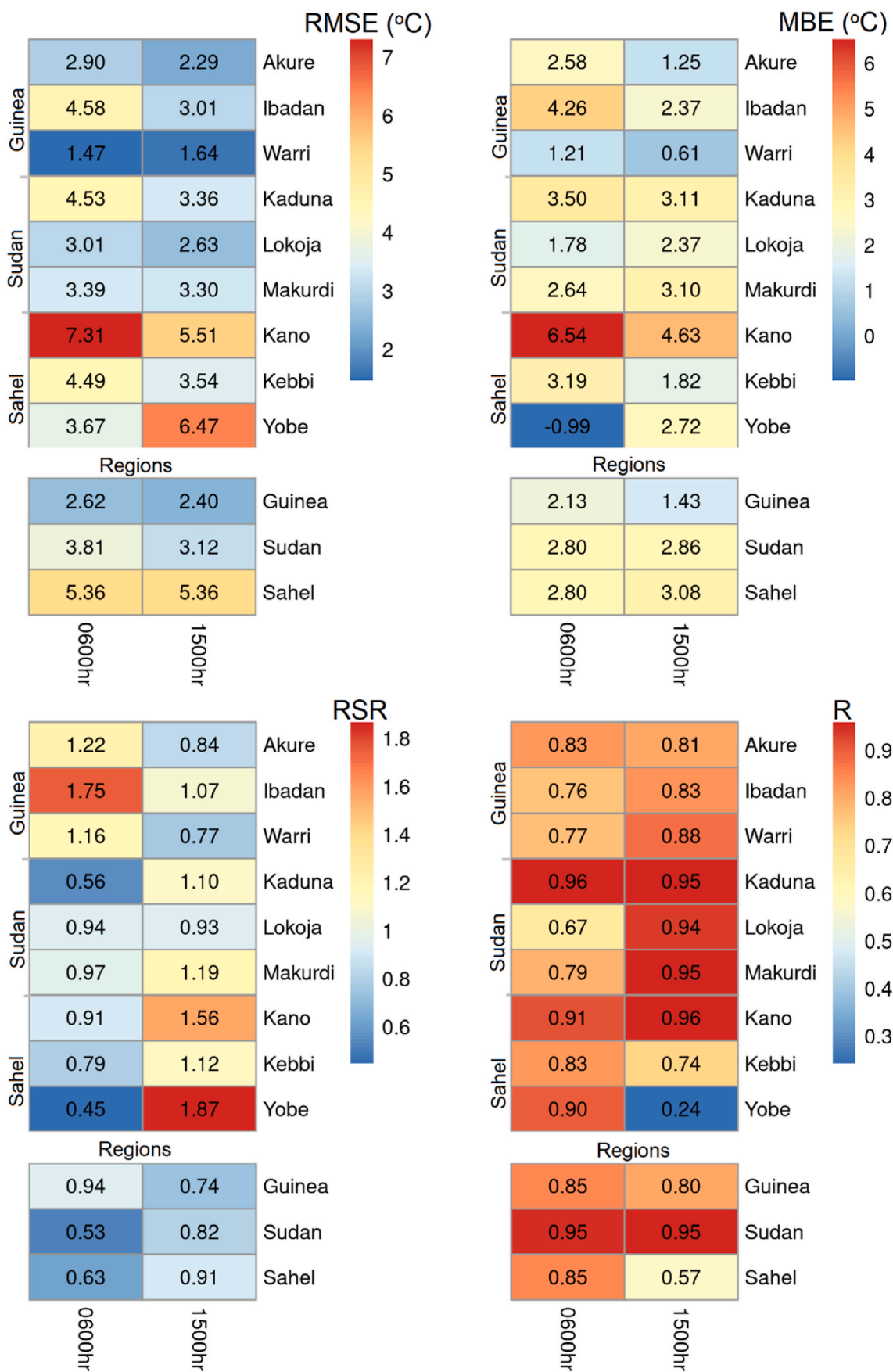


Fig. 3. Performance statistics of monthly ERA5-HEAT across the selected stations and cumulatively for each region, over 1981–2010 for 0 600 and 1 500 LST.

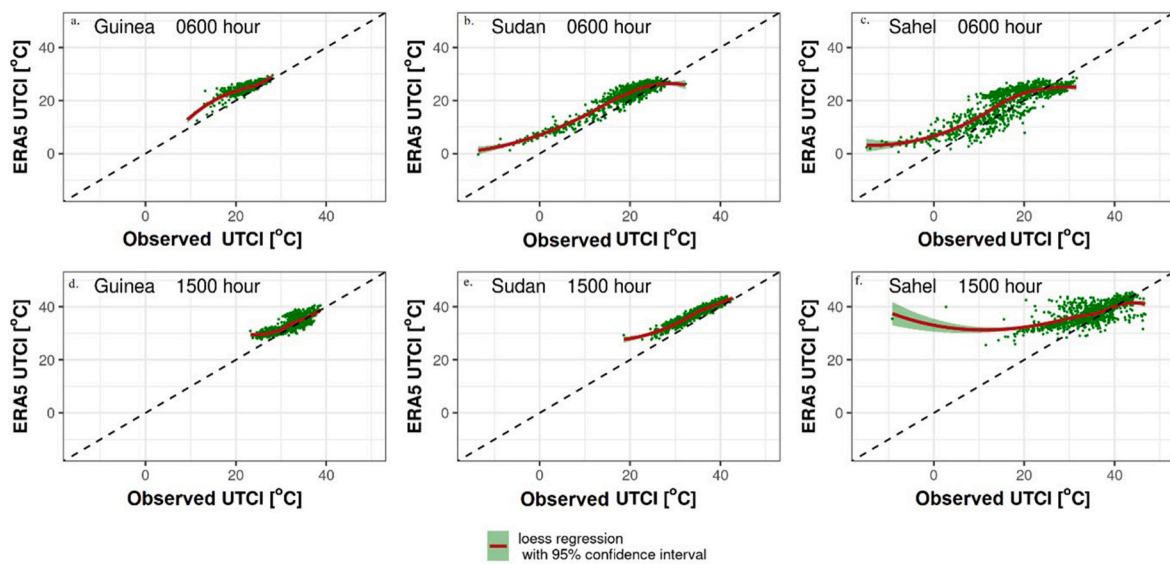


Fig. 4. Scatterplot between ERA5-HEAT and observed (calculated with RayMan) monthly UTCI values across the selected stations, grouped into geographical zones (Guinea, Sudan and Sahel) over 1981–2010 periods for 0 600 and 1 500 LST.

temperature.

Fig. 8 illustrates the spatial coverage of each thermal stress category per decade. The percentage area of SHS in its dominant season drops averagely from 70% to 60 % over a 40-year period, resulting in a rise in the percentage area of VSHS. In the Guinea region, SHS covers about 70% of the area and the rest is covered by MHS and VSHS in DJF and MAM seasons regardless of the year/decade (Fig. 8). The area coverage in other seasons is majorly shared between MHS (50–75 %) and SHS (20–50 %) in the Guinea region regardless of the year/decade. These variations are almost similar for Sudan, but the area coverage of VSHS is relatively higher (80 %) in the MAM season regardless of the year/decade. The cumulative frequency curve further reveals that the area coverage of heat stress in the Sahel is broadly 60–80 % in all seasons, except MAM in which the entire area is covered by VSHS.

Overall, the results reveal the obvious seasonal differences and longitudinal shifts in heat stress levels; more areas experience a higher heat stress levels in MAM than other seasons during the day. These widespread shifts occur notably in the last two decades following the year 2000. Earlier studies using other indices such as ET, RSI and THI (e.g. (Eludoyin et al., 2014)) have reported a significant increase in the spread of thermal stress across Nigeria from 2000 which is in agreement with our study.

3.3. Latitudinal shift in seasonal-decadal UTCI

In this section, we analysed the latitudinal variation of UTCI and the shifts, denoted as Δ UTCI, averaged across the Sahel, Sudan, and Guinea zones longitudinally for the four decades at 0600 and 1500 LST across different seasons. The purpose is to investigate potential changes in latitudinal UTCI variation and identify the precise locations where these changes occur. This analysis is illustrated in Fig. 9.

Generally, at 0600 LST, a consistent latitudinal pattern was observed across the decades per season, and the heat stress category per latitude largely remained unchanged. Although the magnitude of UTCI differed across the seasons at this time, a similar latitudinal pattern was observed in the monsoon months (MAM and JJA) and the drier months (SON and DJF). Evident variation in the latitudinal UTCI occurred in DJF, ranging from 2 to 25 °C, and in SON, it ranged from 11 to 25 °C. In contrast, there was limited variation between 22 and 27 °C observed latitudinally in MAM and JJA, regardless of the decade and year period. Notably, in the last three decades, during MAM, the index increased above the 26.0 °C threshold and changed from the NTS to the MHS around 8–9°N.

Quantitatively, the relative change in UTCI ranged between -0.4 and $+1.5$ °C regardless of the zone and season. However, during DJF, MAM, and JJA seasons, the UTCI shifted in a positive direction over the last three decades (1991–2000, 2001–2010, and 2011–2020) across latitudes, with a stronger magnitude of change observed at higher latitudes. A wider and stronger positive shift was observed in the normally cooler months/season, particularly in DJF, in the Sahel, with an increase of up to 1.5 °C. In the SON season, lower UTCI values were observed in the recent decade, especially in the Sudan region, leading to a negative difference, although not strong enough to effect a thermal categorical change. Overall, across seasons and regions, the changes or shifts have not been large enough to effect a categorical change in thermal classification, except during MAM at around latitude 8–9°N, where the UTCI change resulted in a thermal class change from the NTS to the MHS. A similar situation is expected in the coming decades if the rate of change continues.

At 1500 LST, as earlier mentioned, heat stress level ranges between MHS to VSHS regardless of the latitude and decade (Fig. 9a). However, heterogeneity of heat stress level was observed, that is, transitioning from one heat stress level to another across the latitude was more prevalent unlike at 0600 LST. Also, the seasonal latitudinal pattern shows no similarity of any two seasons implying distinct characteristics of peak time heat stress pattern over the country.

However, UTCI ranges between 28 and 39 °C in both DJF and SON regardless of decade and year period exhibiting similar variability in the drier months. However, it ranges between 31 and 45 °C, and 28–41 °C in MAM and JJA regardless of decade and year period, respectively indicating a similar variability higher than the other two seasons.

Quantitatively, the relative change in decadal averaged UTCI is -0.5 – $(+1.5)$ °C regardless of regions and season. Regionally, in DJF, over Guinea, the UTCI value increased continuously leading to a thermal category change from the MHS to SHS and increased continuously in the Sudan transiting to VSHS in recent three decades. However, in the Sudan region, the UTCI value reduced and changed to SHS, reducing continually into the Sahel region. In the MAM and JJA, the UTCI values increase continuously across the regions changing across thermal categories (Fig. 9b) with the greatest deviation in the MAM. Moreover, in the SON, the UTCI increased and transit from MHS into SHS in Guinea and continued to Sudan. However, a reduction in UTCI was observed around 9°N and a further increase above 11°N in the Sahel was observed. Overall, obvious thermal contrasts exist at 0600 LST and 1500 LST across the latitudinal belt; at 06:00 LST, the UTCI deviation is within

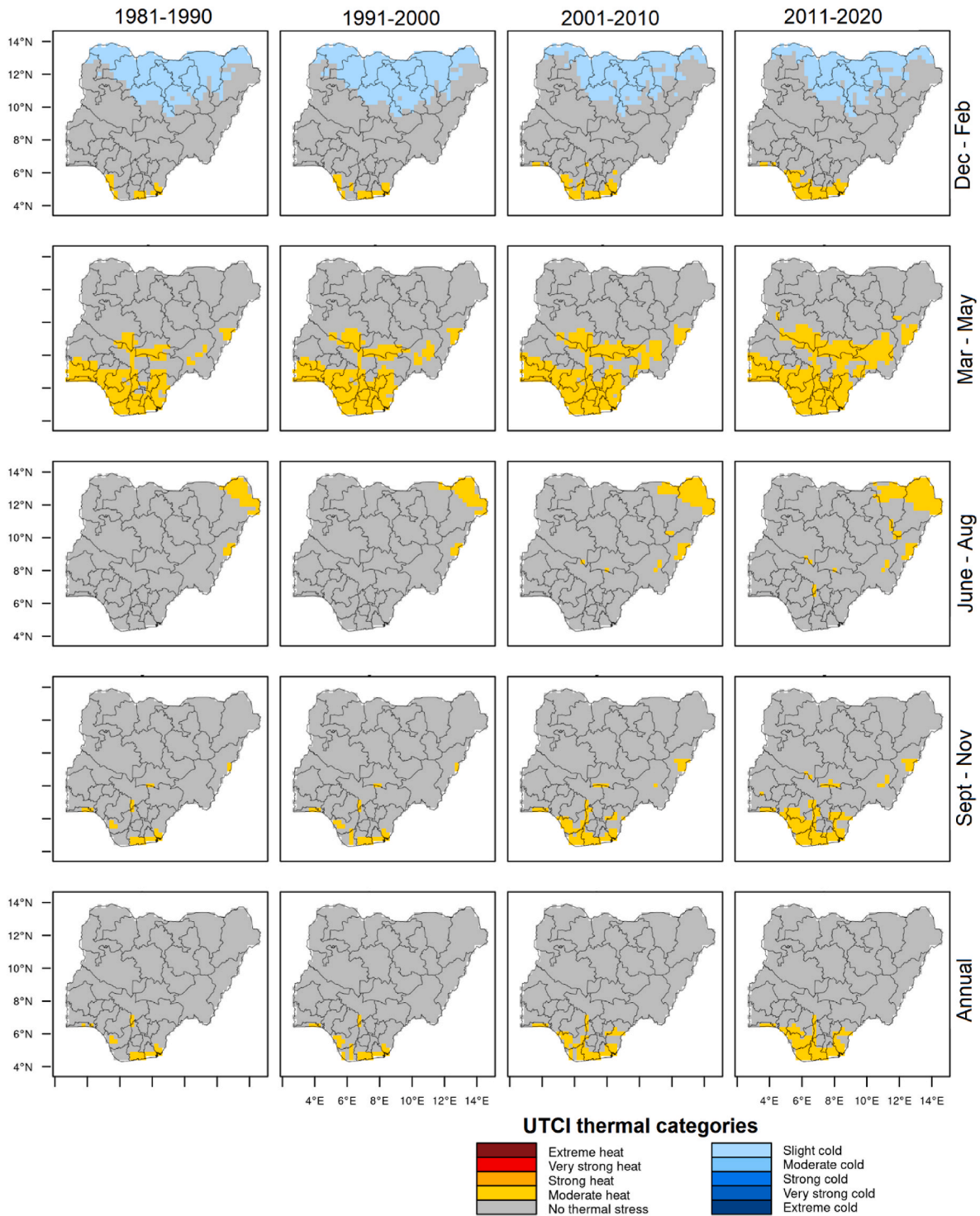


Fig. 5. Spatial, seasonal and decadal characteristics of ERA5-HEAT UTCI at 0 600 LST for the period 1981–2020 over Nigeria.

the NTS zone while 1500 LST revealed a wider deviation spanning three thermal zones (MHS, SHS and VSHS).

3.4. The spatio-temporal trend of ERA5-HEAT UTCI 1981–2020

The spatio-temporal trends of ERA5-HEAT UTCI from 1981 to 2020 are shown in Fig. 10. The results broadly show significant positive trends and occasional non-significant negative trends over the 40-year period. For early morning (0600 LST), the positive trends are relatively higher up to 0.06 °C/year in the Guinea and Sahel region than the Sudan region

in all seasons. The non-significant negative trends up to -0.02 °C/year occur mostly in the Sudan zone around the so-called middle belt region characterised as mountainous, in DJF season. For the hottest afternoon period (1500 LST), the high positive trends occur majorly in DJF and MAM seasons indicating the increasing intensity of heat stress during the peak seasons, and low positive trends in other seasons. On an annual scale, most regions experience elevated thermal stress particularly in the early morning, based on ERA5-HEAT UTCI. The observed positive trends when accumulated over a decade (0.6 °C/decade) are broadly comparable within the range of values (0.2–0.75 °C/decade) reported in

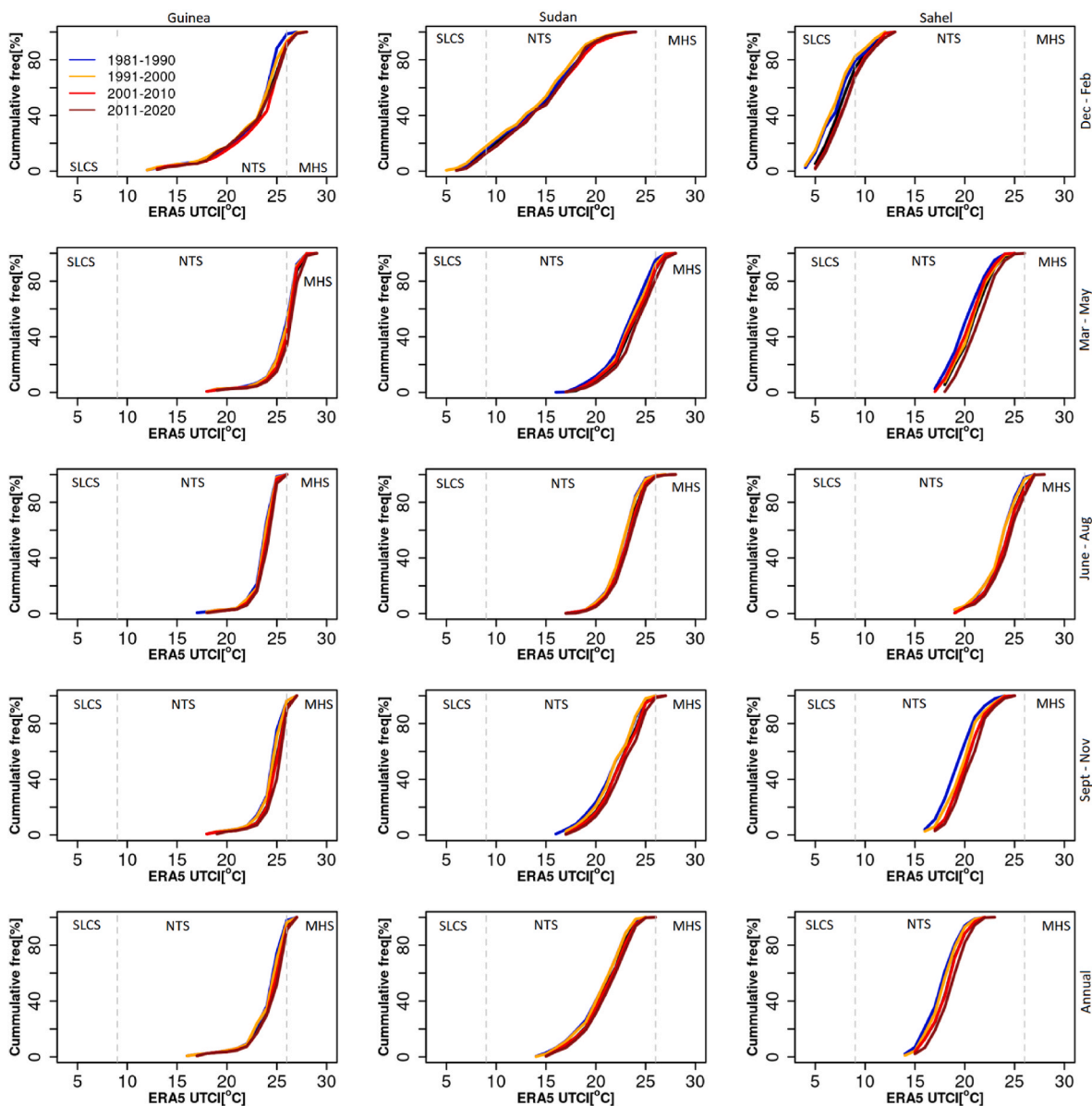


Fig. 6. Cumulative frequency distribution of regional and seasonal ERA-HEAT UTCI values per decade from 1981 to 2020, for 0 600 LST.

related studies (e.g. Shukla et al., 2022; Shukla et al., 2022; Kyaw et al., 2023; Roffe et al., 2023). Such a positive deviation in UTCI has been demonstrated as having adverse effects on human health, including mortality (e.g. Di Napoli et al., 2018).

4. Conclusion

Due to its tropical location, Nigeria is naturally exposed to high solar intensity, leading to warmer temperatures throughout the year. High temperatures, in combination with atmospheric parameters like humidity, wind speed, and mean radiant temperature, determine human thermal comfort and heat stress. This complex phenomenon challenges the body’s ability to maintain an optimal core temperature, affecting comfort, performance, and health. Heat stress has multiple adverse effects on human health, livelihood, and productivity, particularly in terms of health-related impacts, resulting in morbidity and mortality. Unfortunately, knowledge about heat stress is primarily clustered in higher-income regions of the Northern Hemisphere and Australia, leaving tropical and subtropical regions of the global south underrepresented, despite their vulnerability due to poor health infrastructure

and adaptive capacities.

Continuous monitoring of heat stress levels is crucial for early warning and adaptation planning. However, due to limited observation stations and the required instrumentation, a comprehensive characterization of thermal stress in Nigeria and most of sub-Saharan Africa using an energy-based thermal index like UTCI is lacking. Access to near-real-time heat index data, such as ERA5-HEAT UTCI, provides an opportunity to comprehend and monitor heat stress patterns and trends on a large scale, which is vital for countries with low-resolution meteorological networks like Nigeria. However, before adopting this reanalysis product as an alternative to observation in a region, it is essential to conduct a performance evaluation analysis. This study utilizes long-term climate reanalysis data, ERA5-HEAT, to examine the spatio-temporal trends of heat stress across geographic zones in Nigeria. Overall, our findings indicated that ERA5-HEAT exhibits reasonable statistical performance in capturing the temporal characteristics and patterns of UTCI across Nigeria’s different climatic zones. We also observed that the spatial (longitudinal) distribution of heat stress varies by season, encompassing a range from "slightly cold" to "moderate" at 0600 LST and from "moderate" to "very strong" at 1500 LST. Latitudinally, we noticed consistent

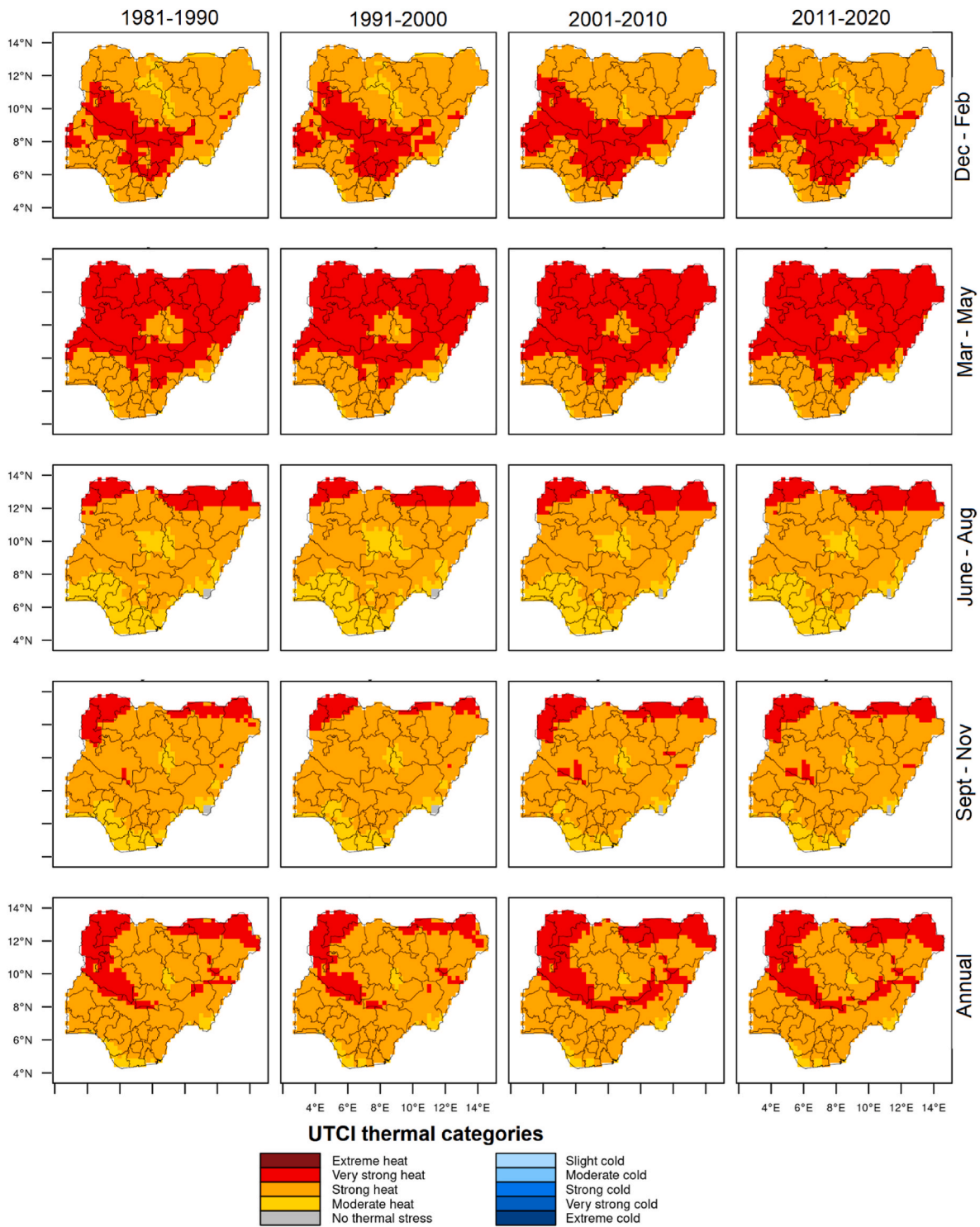


Fig. 7. Spatial, seasonal and decadal characteristics of ERA5-HEAT UTCI at 1 500 LST for the period 1981–2020 over Nigeria.

patterns across decades for each season at 0600 LST, indicating stable heat stress categories. While UTCI values varied by season, a similar latitudinal pattern was observed in both monsoon and drier months. At 1500 LST, more variability in heat stress levels and transitions between categories along latitudes were observed. These seasonal latitudinal patterns were distinct from each other, demonstrating variations in peak-time heat stress across the country. Our long-term spatio-temporal analysis showed a consistent geographical pattern within each season, with March-May (MAM) standing out as a critical period characterized by widespread "very strong" heat stress. Moreover, our results show

significant positive trends over the 40-year period, along with occasional non-significant negative trends. Notably, during the early morning (0600 LST), the positive trends are more pronounced in the Guinea and Sahel regions compared to the Sudan region, regardless of the season. Conversely, during the hottest afternoon period (1500 LST), we observe high positive trends mainly during DJF and MAM seasons, indicating an increase in heat stress intensity during peak seasons, with lower positive trends in other seasons. These positive deviations in UTCI are linked to adverse effects on human health, including increased mortality rates.

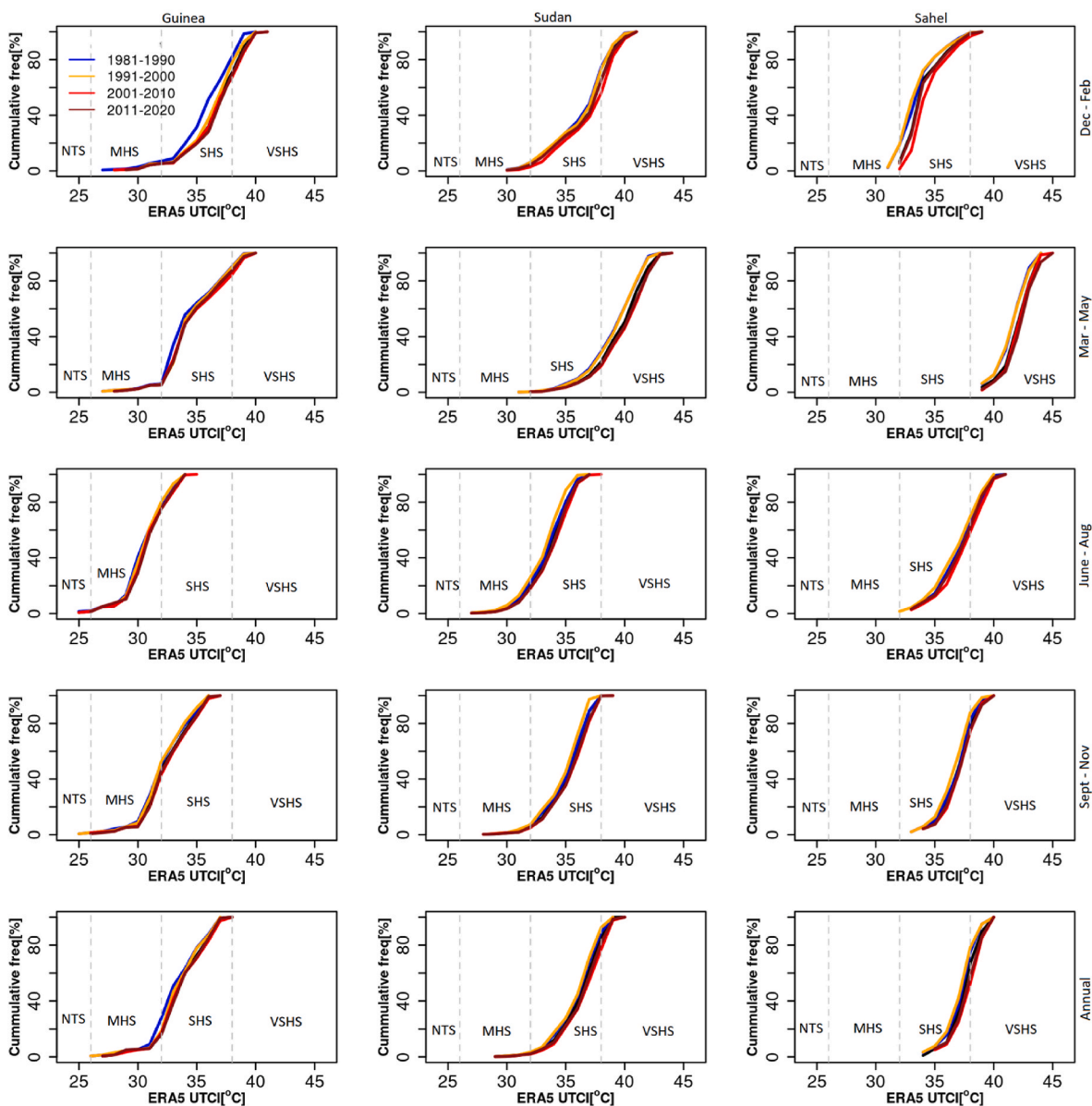


Fig. 8. Cumulative frequency distribution of regional and seasonal ERA-HEAT UTCI values per decade from 1981 to 2020, for 1 500 LST.

While this study has provided context for the application of ERA5-HEAT UTCI datasets as climatological and diagnostic tools for heat stress, it's pertinent to note their potential for driving country or regional-level forecasting systems. The successful prediction of thermal health hazards using UTCI forecasts generated from state-of-the-art Numerical Weather Prediction (NWP) models indicates the maturity of technical capabilities for operational UTCI implementation (Pappenberger et al., 2015). Recently, there has been a rise in UTCI-based forecasting systems in Europe, notably in countries such as the Czech Republic, Italy, Poland, and Portugal, as well as at the pan-European level (Di Napoli et al., 2021b). These systems utilize forecasted variables including air temperature, humidity, wind speed, and mean radiant temperature (MRT) from ECMWF's Integrated Forecasting System (IFS) and further research are required in this regard over Africa in general. Other future work could link heat stress data with vulnerability indicators such as socioeconomic data, average income, public health infrastructure, land use changes, and education levels to develop frameworks for heat risk assessment and adaptation plans. Additionally, future work could examine the influence of different meteorological variables and large-scale atmospheric phenomena, such as the El-Nino

Southern Oscillation, on UTCI in Nigeria. It is also important to extend this study to other global South countries with high heat vulnerability.

CRedit authorship contribution statement

Tobi Eniolu Morakinyo: Conceptualization, Formal analysis, Investigation, Methodology, Project administration, Supervision, Validation, Visualization, Writing – original draft, Writing – review & editing. **Kazeem Abiodun Ishola:** Formal analysis, Investigation, Methodology, Project administration, Supervision, Validation, Visualization, Writing – original draft, Writing – review & editing. **Emmanuel Olaoluwa Eresanya:** Formal analysis, Investigation, Methodology, Validation, Visualization, Writing – original draft, Writing – review & editing. **Mojolaoluwa Toluwalase Daramola:** Formal analysis, Investigation, Methodology, Validation, Visualization, Writing – original draft, Writing – review & editing. **Ifoluwa Adebowale Balogun:** Investigation, Writing – review & editing.

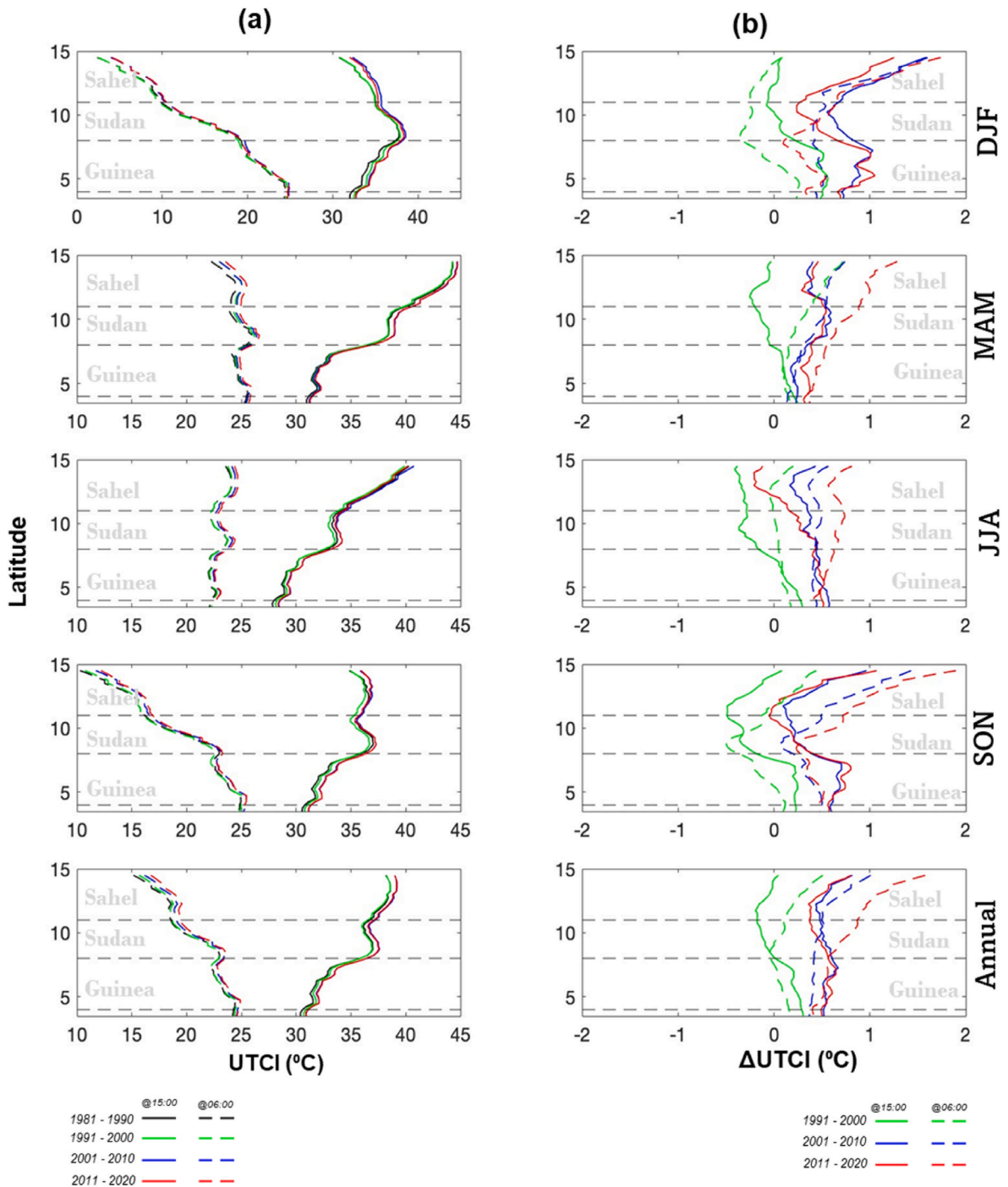


Fig. 9. (a) Averaged UTCI variation between 3 and 15 longitudes for 4 decades from 1981 to 2020, (b) seasonal change in UTCI between the reference period, 1981–1990 and each of the other decade.

Declaration of Generative AI and AI-assisted technologies in the writing process

During the preparation of this work the authors used ChatGPT3.5 in order to grammar check and improve the readability. After using this tool/service, the authors reviewed and edited the content as needed and take(s) full responsibility for the content of the publication.

Declaration of competing interest

The authors declare that they have no known competing financial interests or personal relationships that could have appeared to influence the work reported in this paper.

Data availability

The authors do not have permission to share data.

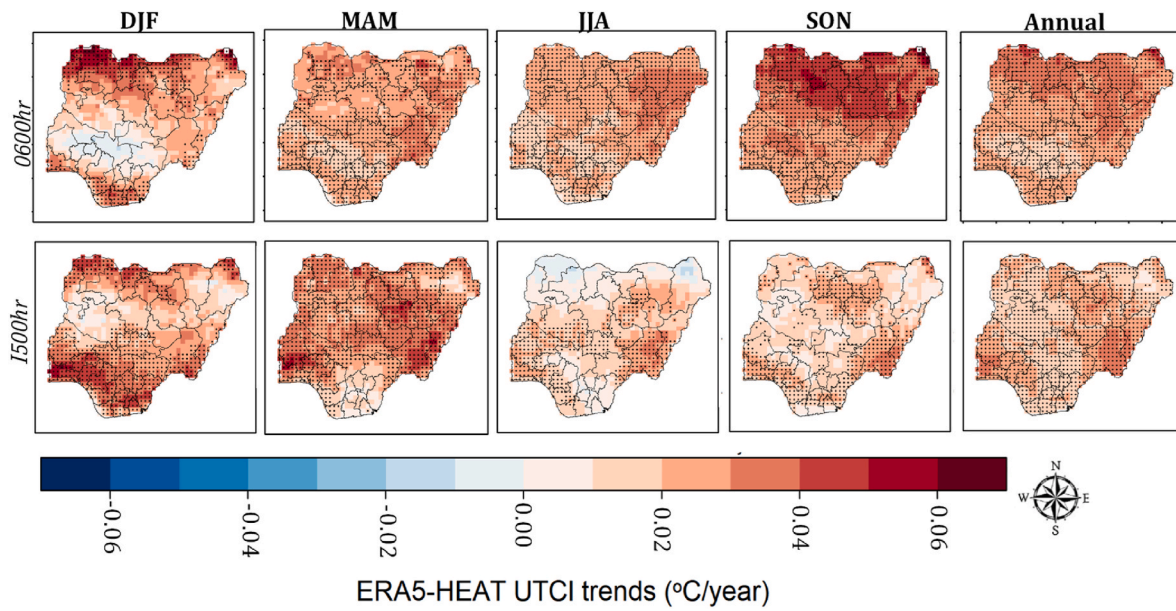


Fig. 10. ERA5-HEAT UTCI trends for 0 600 and 1 500 LST for annual and each season. The stippings represent the grids with statistical significance (p -value < 0.05).

Appendix

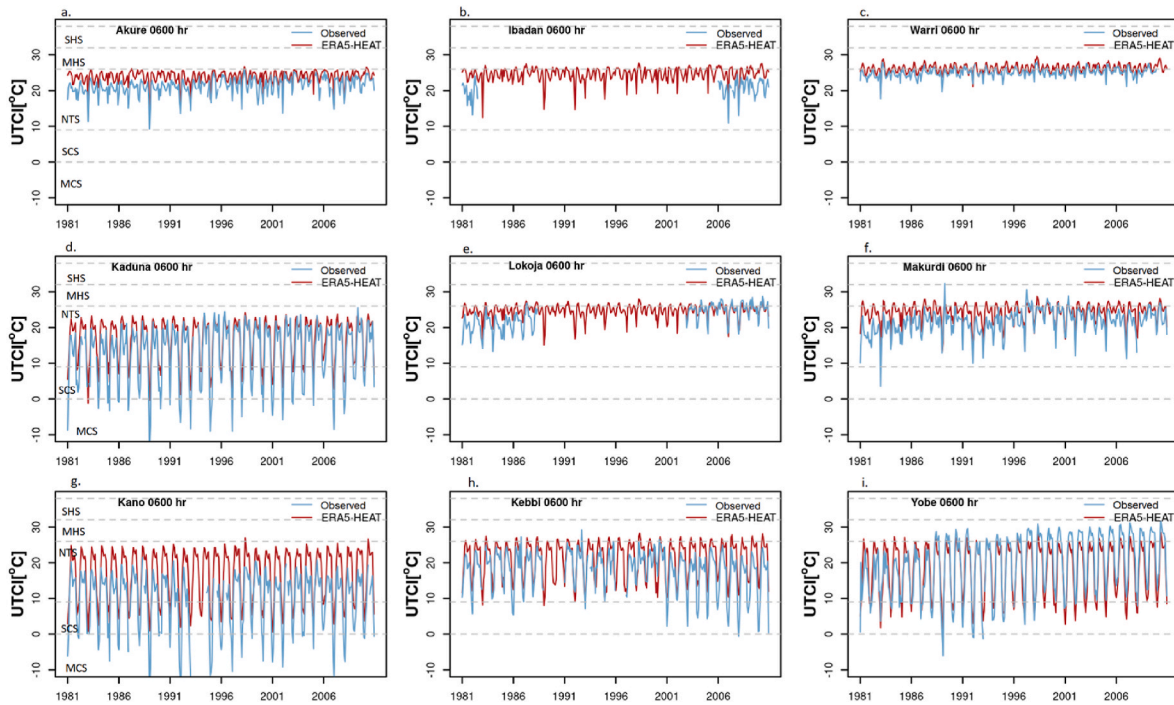


Fig. A1. Temporal comparisons of ERA5-HEAT and observed (calculated with RayMan) monthly UTCI values from 1981 to 2010 across the selected stations, for 0600 LST. The top, mid and bottom rows are for Guinea, Sudan and Sahel stations in that order.

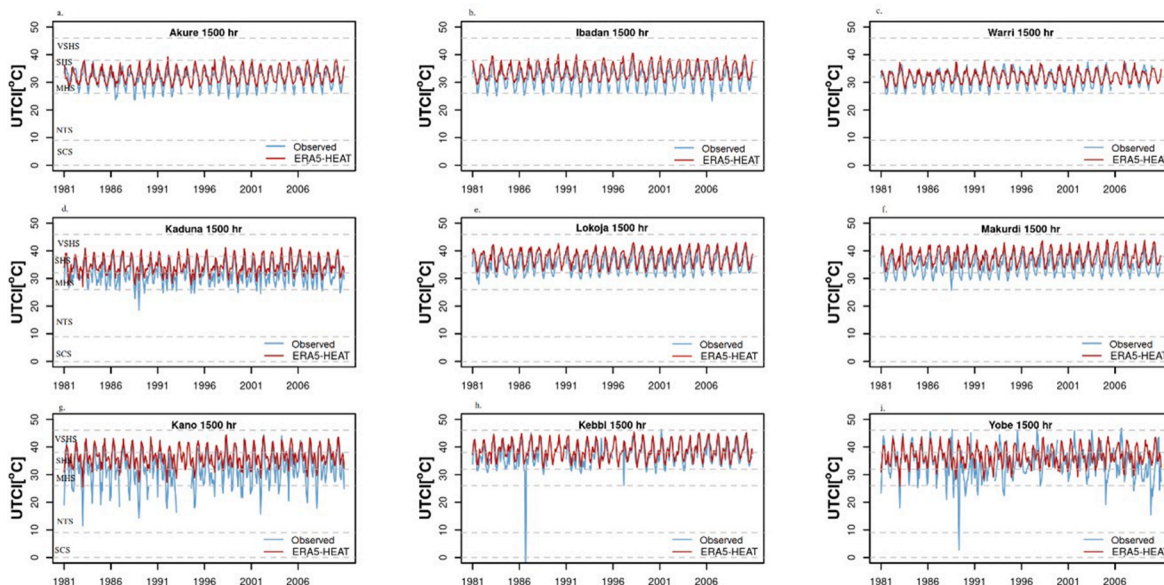


Fig. A2. Temporal comparisons of ERA5-HEAT and observed (calculated with RayMan) monthly UTCI values from 1981 to 2010 across the selected stations, for 1 500 LST. The top, mid and bottom rows are for Guinea, Sudan and Sahel stations in that order.

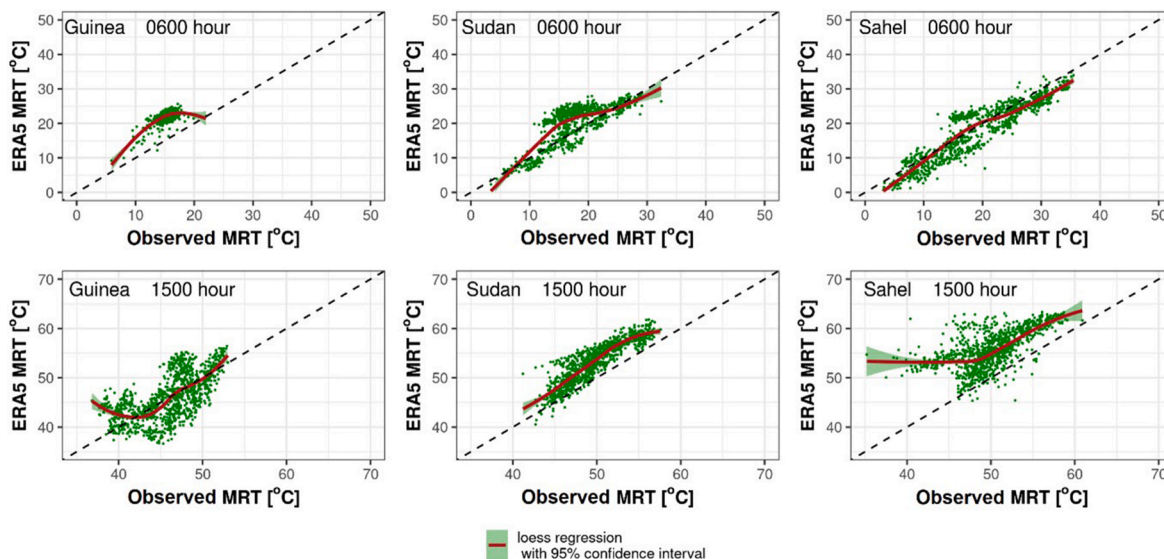


Fig. A3. Scatterplot between ERA5-HEAT and observed (calculated with RayMan) monthly MRT values across the selected stations, grouped into geographical zones (Guinea, Sudan and Sahel) over 1981–2010 periods for 0 600 and 1 500 LST

References

Adegoke, J.O., Ajayi, V.O., 2015. Climate variability and trends in sub-Saharan Africa: a re/view of current and future states. *Int. J. Climatol.* 35 (11), 3529–3559.

Adelekan, I.O., Simpson, N.P., Totin, E., Trisos, C.H., 2022. IPCC Sixth Assessment Report (AR6): Climate Change 2022-Impacts, Adaptation and Vulnerability: Regional Factsheet Africa.

Adeyeri, O.E., Ishola, K.A., 2021. Variability and trends of actual evapotranspiration over West Africa: the role of environmental drivers. *Agric. For. Meteorol.* 308–309 (August), 108574 <https://doi.org/10.1016/j.agrformet.2021.108574>.

Akinsanola, A.A., Ogunjobi, K.O., 2014. Analysis of rainfall and temperature variability over Nigeria. *Global J. Hum. Soc. Sci.: B Geography, Geo-Sciences, Environmental Disaster Management* 14 (3), 1–17.

Amegah, A.K., Rezza, G., Jaakkola, J.J.K., 2016. Temperature-related morbidity and mortality in Sub-Saharan Africa: a systematic review of the empirical evidence. *Environ. Int.* 91, 133–149. <https://doi.org/10.1016/j.envint.2016.02.027>.

Antonescu, B., Mărmureanu, L., Vasilescu, J., Marin, C., Andrei, S., Boldeanu, M., Ene, D., Țileă, A., 2021. A 41-year bioclimatology of thermal stress in Europe. *Int. J. Climatol.* 41 (7), 3934–3952. <https://doi.org/10.1002/joc.7051>.

Ayoade, J.O., 1978. Spatial and Seasonal Patterns of Physiologic Comfort in Nigeria.

Balogun, I.A., Ntekop, A.A., Daramola, M.T., 2019. Assessment of the bioclimatic conditions over some selected stations in Nigeria. *SN Appl. Sci.* 1 (6), 1–14. <https://doi.org/10.1007/s42452-019-0589-y>.

Błażejczyk, K., Jendritzky, G., Bröde, P., Fiala, D., Havenith, G., Epstein, Y., Kampmann, B., 2013. An introduction to the universal thermal climate index (UTCI). *Geogr. Pol.* 86 (1), 5–10.

Bonell, A., Sonko, B., Badjie, J., Samateh, T., Saidy, T., Sosseh, F., Sallah, Y., Bajo, K., Murray, K.A., Hirst, J., Vicedo-Cabrera, A., Prentice, A.M., Maxwell, N.S., Haines, A., 2022. Environmental heat stress on maternal physiology and fetal blood flow in pregnant subsistence farmers in The Gambia, west Africa: an observational cohort study. *Lancet Planet. Health* 6 (12), e968–e976.

Bonell, A., Vicedo-Cabrera, A., Murray, K., Moirano, G., Sonko, B., Moore, S., Haines, A., Prentice, A., 2023. Assessing the impact of heat stress on growth faltering in the first 1000 days of life in rural Gambia, pp. 1–16.

Brimicombe, C., Di Napoli, C., Cornforth, R., Pappenberger, F., Petty, C., Cloke, H.L., 2021. Borderless heat hazards with bordered impacts. *Earth's Future* 9 (9). <https://doi.org/10.1029/2021EF002064>.

Bröde, P., Fiala, D., Błażejczyk, K., Holmér, I., Jendritzky, G., Kampmann, B., Tinz, B., Havenith, G., 2012. Deriving the operational procedure for the universal thermal climate index (UTCI). *Int. J. Biometeorol.* 56 (3), 481–494. <https://doi.org/10.1007/s00484-011-0454-1>.

- Di Napoli, C., Allen, T., Méndez-Lázaro, P.A., Pappenberger, F., 2023. Heat stress in the Caribbean: climatology, drivers, and trends of human biometeorology indices. *Int. J. Climatol.* 43 (1), 405–425. <https://doi.org/10.1002/joc.7774>.
- Di Napoli, C., Barnard, C., Prudhomme, C., Cloke, H.L., Pappenberger, F., 2021a. ERA5-HEAT: a global gridded historical dataset of human thermal comfort indices from climate reanalysis. *Geoscience Data Journal* 8 (1), 2–10. <https://doi.org/10.1002/gdj3.102>.
- Di Napoli, C., Pappenberger, F., Cloke, H.L., 2018. Assessing heat-related health risk in Europe via the universal thermal climate index (UTCI). *Int. J. Biometeorol.* 62 (7), 1155–1165. <https://doi.org/10.1007/s00484-018-1518-2>.
- Di Napoli, C., Messeri, A., Novák, M., Rio, J., Wiczorek, J., Morabito, M., et al., 2021b. The Universal Thermal Climate Index as an operational forecasting tool of human biometeorological conditions in Europe. Applications of the Universal Thermal Climate Index UTCI in Biometeorology: Latest Developments and Case Studies, pp. 193–208.
- Eludoyin, O.M., 2014. A perspective of the diurnal aspect of thermal comfort in Nigeria. *Atmos. Clim. Sci.* 4 (4), 696–709. <https://doi.org/10.4236/acs.2014.44063>.
- Eludoyin, O.M., Adelekan, I.O., 2013. The physiologic climate of Nigeria. *Int. J. Biometeorol.* 57 (2), 241–264. <https://doi.org/10.1007/s00484-012-0549-3>.
- Eludoyin, O.M., Adelekan, I.O., Webster, R., Eludoyin, A.O., 2014. Air temperature, relative humidity, climate regionalization and thermal comfort of Nigeria. *Int. J. Climatol.* 34 (6), 2000–2018. <https://doi.org/10.1002/joc.3817>.
- Eresanya, E.O., Ajayi, V.O., Daramola, M.T., Balogun, R., 2018. Temperature extremes over selected stations in Nigeria. *Phys. Sci. Int. J.* 20, 1–10. <https://journalpsij.com/index.php/PSIJ/article/view/541/1081>.
- Evans, J.S., Murphy, M.A., Ram, K., 2020. *spatialEco: Spatial Analysis and Modelling Utilities*, 2021.
- Fiala, D., Havenith, G., Bröde, P., Kampmann, B., Jendritzky, G., 2012. UTCI-Fiala multi-node model of human heat transfer and temperature regulation. *Int. J. Biometeorol.* 56 (3), 429–441. <https://doi.org/10.1007/s00484-011-0424-7>.
- Fröhlich, D., Gangwisch, M., Matzarakis, A., 2019. Effect of radiation and wind on thermal comfort in urban environments - application of the RayMan and SkyHelios model. *Urban Clim.* 27, 1–7. <https://doi.org/10.1016/j.uclim.2018.10.006>. September 2018.
- Gbode, I.E., Adeyeri, O.E., Menang, K.P., Intsiful, J.D., Ajayi, V.O., Omotosho, J.A., Akinsanola, A.A., 2019. Observed changes in climate extremes in Nigeria. *Meteorol. Appl.* 26 (4), 642–654.
- Guigma, K.H., Todd, M., Wang, Y., 2020. Characteristics and thermodynamics of Sahelian heatwaves analysed using various thermal indices. *Clim. Dynam.* 55 (11–12), 3151–3175.
- Havenga, H., Coetzee, B., Burger, R.P., Piketh, S.J., 2022. Increased risk of heat stress conditions during the 2022 Comrades Marathon. *South Afr. J. Sci.* 118 (7–8), 1–5. Kendall, M.G., 1948. Rank Correlation Methods.
- Krüger, E.L., Di Napoli, C., 2022. Feasibility of climate reanalysis data as a proxy for onsite weather measurements in outdoor thermal comfort surveys. *Theor. Appl. Climatol.* 149 (3–4), 1645–1658. <https://doi.org/10.1007/s00704-022-04129-x>.
- Kyaw, A.K., Hamed, M.M., Shahid, S., 2023. Spatiotemporal changes in universal thermal climate index over South Asia. *Atmos. Res.* 292 <https://doi.org/10.1016/j.atmosres.2023.106838>.
- Mann, H., 1945. Non-parametric tests against trend. *Econometrica. MathSci Net* 13, 245–259.
- Matzarakis, A., Rutz, F., Mayer, H., 2007. Modelling radiation fluxes in simple and complex environments - application of the RayMan model. *Int. J. Biometeorol.* 51 (4), 323–334. <https://doi.org/10.1007/s00484-006-0061-8>.
- Matzarakis, A., Rutz, F., Mayer, H., 2010. Modelling radiation fluxes in simple and complex environments: basics of the RayMan model. *Int. J. Biometeorol.* 54 (2), 131–139. <https://doi.org/10.1007/s00484-009-0261-0>.
- Miranda, V.F.V.V., Müller, G.V., Thielend, D., Libonati, R., 2023. Heat stress in South America over the last four decades: a bioclimatic analysis. <https://doi.org/10.21203/rs.3.rs-3029614/v1>.
- Morakinyo, T.E., Ogungbenro, S.B., Abolude, A.T., Akinsanola, A.A., 2019. Quantifying the effect of rain events on outdoor thermal comfort in a high-density city, Hong Kong. *Int. J. Biometeorol.* 63 (1) <https://doi.org/10.1007/s00484-018-1634-z>.
- Ncongwane, K.P., Botai, J.O., Sivakumar, V., Botai, C.M., 2021. A literature review of the impacts of heat stress on human health across africa. *Sustainability* 13 (9). <https://doi.org/10.3390/su13095312>.
- Nicholson, S.E., 2013. The West African Sahel: A review of recent studies on the rainfall regime and its interannual variability. *Int. Sch. Res. Notices* 2013 (1), 453521.
- Nikulin, G., Jones, C., Giorgi, F., Asrar, G., Büchner, M., Cerezo-Mota, R., Sushama, L., 2012. Precipitation climatology in an ensemble of CORDEX-Africa regional climate simulations. *J. Clim.* 25 (18), 6057–6078.
- Ogbonna, A.C., Harris, D.J., 2008. Thermal comfort in sub-Saharan Africa: field study report in Jos-Nigeria. *Appl. Energy* 85 (1), 1–11. <https://doi.org/10.1016/j.apenergy.2007.06.005>.
- Okeahialam, B.N., 2016. Article commentary: the cold dusty harmattan: a season of anguish for cardiologists and patients. *Environ. Health Insights* 10, 143–146. <https://doi.org/10.4137/EHI.S38350>.
- Olaniran, O.J., 1982. The physiological climate of Ilorin, Nigeria. *Archives for Meteorology, Geophysics, and Bioclimatology Series B.* <https://doi.org/10.1007/BF02278298>.
- Oluleye, A., Adeyewa, D., 2016. Wind energy density in Nigeria as estimated from the ERA interim reanalysed data set. *Current Journal of Applied Science and Technology* 17 (1), 1–17. <https://doi.org/10.9734/BJAST/2016/13340>.
- Omonijo, A.G., 2017. Assessing seasonal variations in urban thermal comfort and potential health risks using Physiologically Equivalent Temperature: a case of Ibadan, Nigeria. *Urban Clim.* <https://doi.org/10.1016/j.uclim.2017.05.006>.
- Omonijo, A.G., Adeofun, C.O., Oguntoko, O., Matzarakis, A., 2013. Relevance of thermal environment to human health: a case study of Ondo State, Nigeria. *Theor. Appl. Climatol.* 113 (1–2), 205–212. <https://doi.org/10.1007/s00704-012-0777-9>.
- Omotosho, J.B., Abiodun, B.J., 2007. A numerical study of moisture build-up and rainfall over West Africa. *Meteorol. Appl.* 14 (3), 209–225. <https://doi.org/10.1002/met.11>.
- Parkes, B., Buzan, J.R., Huber, M., 2022. Heat stress in Africa under high intensity climate change. *Int. J. Biometeorol.* 66 (8), 1531–1545. <https://doi.org/10.1007/s00484-022-02295-1>.
- Pasquini, L., van Aardenne, L., Godsmark, C.N., Lee, J., Jack, C., 2020. Emerging climate change-related public health challenges in Africa: a case study of the heat-health vulnerability of informal settlement residents in Dar es Salaam, Tanzania. *Sci. Total Environ.* 747 <https://doi.org/10.1016/j.scitotenv.2020.141355>.
- Pappenberger, F., Jendritzky, G., Staiger, H., Dutra, E., Di Giuseppe, F., Richardson, D.S., Cloke, H.L., 2015. Global forecasting of thermal health hazards: the skill of probabilistic predictions of the Universal Thermal Climate Index (UTCI). *Int. J. Biometeorol.* 59, 311–323.
- Roffe, S.J., van der Walt, A.J., Fitchett, J.M., 2023. Spatiotemporal characteristics of human thermal comfort across southern Africa: an analysis of the Universal Thermal Climate Index for 1971–2021. *Int. J. Climatol.* 43 (6), 2930–2952. <https://doi.org/10.1002/joc.8009>.
- Runnalls, K.E., Oke, T.R., 2000. Dynamics and controls of the near-surface heat island of Vancouver, British Columbia. *Phys. Geogr.* 21 (4), 283–304.
- Santamouris, M., 2015. Analyzing the heat island magnitude and characteristics in one hundred Asian and Australian cities and regions. *Sci. Total Environ.* 512, 582–598.
- Sen, P.K., 1968. Estimates of the regression coefficient based on Kendall's tau. *J. Am. Stat. Assoc.* 63 (324), 1379–1389.
- Shukla, K.K., Attada, R., Kumar, A., Kunchala, R.K., Sivareddy, S., 2022. Comprehensive analysis of thermal stress over northwest India: climatology, trends and extremes. *Urban Clim.* 44 <https://doi.org/10.1016/j.uclim.2022.101188>.
- Soneye, O.O., Ayoola, M.A., Ajao, I.A., Jegede, O.O., 2019. Diurnal and seasonal variations of the incoming solar radiation flux at a tropical station, Ile-Ife, Nigeria. *Heliyon* 5 (5), e01673.
- Sultan, B., Janicot, S., Diedhiou, A., 2003. The West African monsoon dynamics. Part I: documentation of intraseasonal variability. *J. Clim.* 16 (21), 3389–3406.
- Trisos, C.H., Adelekan, I.O., Totin, E., Ayanlade, A., Efitre, J., Gameda, A., Kalaba, K., Lennard, C., Masao, C., Mgaya, Y., others, 2022. Nine principles for encouraging a context-driven, inclusive and proactive approach to planning for climate risk in African cities. *Climate Change 2022: Impacts, Adaptation and Vulnerability*.
- Tuholske, C., Caylor, K., Funk, C., Verdin, A., Sweeney, S., Grace, K., Peterson, P., Evans, T., 2021. Global urban population exposure to extreme heat. *Proc. Natl. Acad. Sci. U.S.A.* 118 (41), 1–9. <https://doi.org/10.1073/pnas.2024792118>.
- UNDESA, 2019. United Nations Department of Economic and Social Affairs. *Population Division. World Population Prospects*.
- Urban, A., Di Napoli, C., Cloke, H.L., Kysely, J., Pappenberger, F., Sera, F., Schneider, R., Vicedo-Cabrera, A.M., Acquaotta, F., Ragetti, M.S., Íñiguez, C., Tobias, A., Indermitte, E., Orru, H., Jaakkola, J.J.K., Rytli, N.R.I., Pascal, M., Huber, V., Schneider, A., et al., 2021. Evaluation of the ERA5 reanalysis-based universal thermal climate index on mortality data in Europe. *Environ. Res.* 198 <https://doi.org/10.1016/j.envres.2021.111227>.
- VDI, 1998. *Methods for the Human Biometeorological Evaluation of Climate and Air Quality for the Urban and Regional Planning at Regional Level*. VDI, Berlin, Germany, p. 3787.
- World Bank, 2021. Nigeria. Current climate: climatology. <https://climateknowledgeportal.worldbank.org/country/nigeria/climate-data-historical#:~:text=Nigeria%20is%20characterized%20by%20three,amounts%20from%20south%20to%20north>. (Accessed 7 May 2024).
- Zare, S., Hasheminejad, N., Shirvan, R., Hemmatjo, H.E., Sarebanzadeh, K., Ahmadi, S., 2018. Comparing universal thermal climate index (UTCI) with selected thermal indices/environmental parameters during 12 months of the year. *Weather Clim. Extrem.* 19, 49–57. <https://doi.org/10.1016/j.wace.2018.01.004>.
- Zhao, Q., Guo, Y., Ye, T., Gasparrini, A., Tong, S., Overcenco, A., Urban, A., Schneider, A., Entezari, A., Vicedo-Cabrera, A.M., Zanobetti, A., Analitis, A., Zeka, A., Tobias, A., Nunes, B., Alahmad, B., Armstrong, B., Forsberg, B., Pan, S.C., Li, S., 2021. Global, regional, and national burden of mortality associated with non-optimal ambient temperatures from 2000 to 2019: a three-stage modelling study. *Lancet Planet. Health* 5 (7), e415–e425. [https://doi.org/10.1016/S2542-5196\(21\)00081-4](https://doi.org/10.1016/S2542-5196(21)00081-4).